

EVALUATION OF A HIGH TEMPERATURE ADHESIVE FOR FABRICATING GRAPHITE/PMR-15 POLYIMIDE STRUCTURES

S.G. Hill and J.B. Cushman
Boeing Aerospace Company

Tests were conducted to measure shear strength, shear modulus and flatwise tensile strength of A7F (amide-imide modified LARC-13) adhesive system. An investigation was also conducted to determine the effect of geometric material parameters, and elevated temperature on the static strength of "standard" joints. Single-lap and double-lap composite joints, and single, double and step lap composite to metal joints were characterized. A series of advanced joints consisting of preformed adherends, adherends with scalloped edges and joints with hybrid interface plies were tested and compared to baseline single and double-lap designs.

INTRODUCTION

Graphite/polyimide composites have shown potential for use as a structural material at elevated temperatures on advanced aerospace vehicles. Unlike typical graphite/epoxy systems which are limited to 300° - 350°F operating range, graphite/polyimide systems can operate in the 500 - 600°F range. This characteristic makes graphite/polyimide systems attractive for use in high Mach number missiles and space shuttle type transportation systems where, depending on configuration, location, and thermal protection system, temperatures greater than 500°F could be experienced.

To evaluate a high temperature adhesive for fabricating graphite/PMR-15 polyimide structures, a test program was conducted to evaluate A7F polyimide adhesive for bonding metal-to-metal, metal to composite, and composite-to-composite joints. The A7F adhesive was formulated by Boeing using LARC-13 adhesive furnished by NASA Langley. U.S. Polymeric, Inc. coated the A7F adhesive on 112 E-glass/A-1100 scrim to make film adhesive. Three environmental conditions for the adhesive tests were examined: 1) as cured/past cured, 2) soaked for 125 hours at 589°K (600°F) in a one (1) atmosphere environment (air), and thermally cycled 125 times in a temperature range from 116°K to 589°K (-250 - 600°F). Test for the standard joints and advanced joints ranged from 116K - 561K (-250°F - 550°F).

MATERIAL

The high temperature adhesive characterized in this study is designated A7F. A7F is a 50:50 resin solids copolymer blend of LARC-13 adhesive (supplied by NASA, Langley) (Ref. 1) and AMOCO's AI 1130 Amide-Imide. Sixty percent by weight aluminum powder and 5% by weight Cab-O-sil are added. The adhesive was applied to 112E glass/A-1100 scrim to form a .25mm (.01 in.) thick adhesive film.

Preceding page blank

The high temperature composite materials characterized under the study were laminates of graphite/polyimide tape materials. Based on previous experience from the CASTS* program research, Boeing and NASA chose the celion/PMR-15 material system. The graphite fiber was CE 3000, with NR150B2G polyimide sizing. Preimpregnated tape was procured from U.S. Polymeric, Inc. to a material specification contained in Reference 2. Gr/PI and S-glass/PI fabric used in the advance joints were preimpregnated in the Boeing Materials Technology Laboratory utilizing resin from the same batch that was used to impregnate the tape material. The titanium used was Ti-6Al-4V (standard) per MIL-T-9046, Type III, Composition C.

SPECIMEN FABRICATION - ADHESIVE TESTS

Specimens for the adhesive test were fabricated in the laboratory using standard laboratory practices. Titanium surfaces were chromic acid anodized and primed with a dilute solution of the A7F adhesive. Specimens were assembled to the configurations in Figures 1-3 using A7F film adhesive and cured using the procedures in Reference 2.

SPECIMEN FABRICATION - BONDED JOINT TESTS

The composite adherends were laminates of graphite fibers impregnated with PMR-15 resin. The fibers were sized with NR150B2G. Special requirements were imposed upon the prepreg supplier (U.S. Polymeric, Inc.) that limited the size of resin batches mixed to 24 lb. maximum. This was to limit the exothermic reaction during mixing. Prepreg was fabricated from one fiber lot. Because of limits on resin batch size, more than one batch of resin was needed to make the required amount of prepreg; therefore, quality control tests were conducted on any prepreg roll that was made from a different resin batch. Chemical characterization tests were also conducted using high pressure liquid chromatography, gas chromatography, mass spectroscopy, infrared spectroscopy, and thermal gravimetric analysis.

Panels fabricated from the prepreg were cured according to the cure cycle in Reference 2. All panels were non-destructively inspected. The procedure used was C-scan at 5-6 MHz sweep at 4 db loss above the water path. Laminates containing voids or other defects greater than .06 in² were rejected for use in this study. Once the panel had passed C-scan, the panels were ready for preparation for bonding. The panels were primed and bonded with A7F adhesive per the procedure in Reference 2.

Effect of Conditioning on Specimens

Three environmental conditioning cycles were used in this study. Conditioning code numbers were assigned to the specimens as follows:

Condition 1 As cured/post cured

*Composites for Advanced Space Transportation Systems (Contract NAS1-15009 & NAS1-15644).

- Condition 2 Aged for 125 hrs and at 589K (600°F) in a 1 atm environment (air)
- Condition 3 Thermally cycled 125 times -116K (-250°F) - -589K (600°F) in an one (1) atmosphere environment (air). The cryogenic temperature of -250°F was held for one half (1/2) hr and the maximum temperature was held for one (1) hour per cycle.

The conditioning cycles did not exhibit a significant effect on the specimens. The specimens tested at the 561K (550°F) displayed better properties than specimens tested at 116K (-250°F).

Adhesive Test Results

Average test results for the 12.7 mm (0.5 in.) single lap shear, "thick adherend" shear and flatwise tension tests are shown in Table 6-1 for the various conditionings and test temperatures.

Since the "thick adherend" test specimen has lower peel stresses than the standard single lap specimens, it was expected that the shear strengths from this test would be higher than those from the titanium lap shear (ASTM D 1002) tests. Results for cured/post-cured specimens at 294K (70°F) and 561K (550°F) are higher for the ASTM D 1002 procedure than for the "thick adherend" procedure. ASTM D 1002 results for aged specimens were slightly higher than "thick adherend" results at 561K (550°F).

There is no known explanation for these anomalies other than possible material and processing variations. C-scans of the bond lines showed no defects. Adhesive thicknesses could have been different for the two specimen configurations. Also there may have been some edge effects during the curing or aging. The thick adherend specimens were conditioned as a single plate approximately 508 mm (20 in.) wide and then cut into specimens. The ASTM D 1002 specimens were made from standard titanium "finger" blanks 25.4 mm (1.0 in.) wide which may have contributed to edge effects.

The average shear modulus from the "thick adherend" tests was 58 MPa (8000 psi) with the data showing drops in moduli at both cryogenic and elevated temperature with respect to room temperature. The room temperature aged specimens exhibited a bimodulus behavior. Results from the same tests show a decrease in ultimate shear strain with increasing temperature.

Flatwise (out-of-plane) tension tests were conducted on cured/post-cured specimens that had stainless steel rods, while the aged specimens had titanium rods. All specimens failed cohesively. Test results show a drop in strength with an increase in temperature. On the average, flatwise tension strength for A7F adhesive are twice that for a Celion 3000/PMR-15 laminate (Ref. 3). This indicates that joints with strengths governed by peel failures will fail in the laminate rather than in the adhesive.

Results of coefficient of thermal expansion (CTE) tests on A7F adhesive conducted under contract TASK 1.2.1 (Ref. 3) are shown in Figure 4. Data show a significant drop in CTE due to aging.

Standard Joint Test Results

Test results obtained for the single- and double-lap joints had a significant amount of data scatter. Therefore, comparisons between joint types are based on average failure loads only.

In most cases the "Gr/PI-Gr/PI" joints exhibited an intralamina failure mode caused by peel stresses in the composite adherends as shown in Figure 5. This failure mode consists of a failure within a ply, as opposed to an interlamina mode where the failure occurs between plies. For both single- and double-lap joints, the intralamina failure occurred in the ply nearest the joint interface, with the failure occurring for the double-lap joint in the inner adherends.

The "Gr/PI-titanium" specimens also exhibited intralamina and/or interlamina failures in the plies near the joint interface; however, some specimens also had adhesive failures over a portion of the joint. Evidence of partial adhesive failure occurred at all test temperatures but was predominant at the elevated temperature.

Failure loads versus lap length for single- and double-lap "Gr/PI-Gr/PI" and "Gr/PI-titanium" joints are shown in Figures 5 and 6 respectively. As expected there was a general increase in failure load with increasing lap length, with the loads appearing to approach asymptotes.

Results for the "3-step" symmetric step-lap joints are shown in Figure 8. As was expected there is a strong temperature dependence in the strength of these joints. This is attributable to the difference in coefficients of thermal expansion between the Gr/PI and titanium adherends and the elevated cure temperature, which result in residual thermal stresses in the joint and thus decreased strength at lower temperatures.

A comparison of "Gr/PI-titanium" double lap joints with the "3-step" symmetric step-lap joint shows them to be about equal in strength for the lap lengths tested. At these load levels a double-lap joint would be the better design solution because of simplicity in manufacturing (other design constraints such as fatigue resistance, surface smoothness or weight may not allow this). Higher loads would dictate a symmetric step-lap (with more than 3 steps) or a scarf joint since increasing the lap length of a double-lap joint would not result in any significant additional strength.

In general, failure loads for the standard joints increased with increasing temperature, with the change in loads from cryogenic to room temperature being less than the change in loads from room to elevated temperature.

The maximum joint loads achieved in the standard joint test program are summarized in Figure __. The maximum load achieved for a single-lap joint (25.4 mm (1.0 in.) wide) was 9.71 kN (2184 lb) while for the double-lap and step-lap joints (25.4 mm (1.0 in.) wide) it was 24.64 kN (5540 lb) and 22.89 kN (5147 lb) respectively. All three maximums occurred at a test temperature of 561K (550°F). Maximum loads shown should not be construed to be the maximum obtainable. Other layouts or joint configurations for a particular joint type could have resulted in higher failure loads.

Advanced Joint Test Results

Results of the preformed adherend tests demonstrate that preforming the adherends of a single-lap joint gives a significant increase in load carrying capability. Figures 11 and 12 show the effect of preforming for temperatures of 294K (70°F) and 561K (550°F). The average failure load for each lap length is normalized by the average failure load for the baseline (straight adherends) configuration (from the advanced joint test matrix) with the same lap length. In all cases, preforming the adherends increased the average failure load. Increases ranged from 92% to 262% at 294K (70°F) and from 46% to 234% at 561K (550°F). No comparisons were made at 116K (-250°F) because there was no baseline data at this temperature; however, results similar to the 294K (70°F) tests would be expected.

In contrast to the standard joints, the preformed adherend specimens had failure loads at elevated temperature which were in all cases lower than those at room temperature. The results for the 116K (-250°F) specimens were not as consistent; with some values falling above the room temperature loads, some values between the room and elevated temperature loads and in some values below the elevated temperature failure loads. These results may be in part due to the large scatter in the failure load data.

Several failure modes were exhibited by the preformed adherend specimens as outlined in Table 2. The failure modes changed from a purely intralaminar peel failure in the ply next to the joint interface, to severe delaminations and peel failures through the adherend thickness, to a failure outside of the joint at the preform bend as the lap lengths and preform angles increased. This change in failure modes may explain why the longer lap length specimens showed smaller improvements in strength over the baseline joints than the shorter lap length specimens (see Figs. 11 and 12). This result was the reverse of that expected from the results of testing by Sawyer and Cooper (Ref. 4).

Scalloping the single-lap joints gave a slight drop in failure load while scalloping the double-lap joints resulted in an average increase of 17% in failure load. The difference between these two cases can be attributed to the different failure mechanisms of a single versus double-lap joint. The failure in a single-lap joint is governed by both the moment introduced in the joint and by peel stresses. The failure in the double-lap joints is governed primarily by the peel stresses in the inner adherend at the end of the lap. Since scalloping the ends of the adherends was designed to reduce the peel stresses at the end of the lap, it would be expected that the double-lap joints would be more affected by scalloping than single-lap joints.

Failure loads versus lap length for the Gr/PI fabric interface, and S-glass fabric interface specimens tested at room and elevated temperature are compared to baseline data in Figures 13 and 14. Placing fabric interfaces, S-glass/PI and Gr/PI, between the single-lap joint adherends resulted in 28% to 76% increases in average failure load (see Table 8-2) except for the 25.4 mm (1.0 in.) lap length S-glass/PI specimens, which showed no significant change in strength. The increase in strength can be attributed to a reduction in peak shear and peel stresses due to the "softer" interface materials. Most of the fabric interface specimens delaminated between the two fabric plies, as opposed to delaminating in the adherends as was the case for the standard joints.

The temperature dependence of the joint strengths for the scalloped adherend and fabric interface joints was less than that for the standard joints. In general, there was no significant difference between the failure loads for the room and elevated temperature cases for these joints, with the average difference being a 5% increase from room to elevated temperature. For the few cases where there was a significant difference the elevated temperature loads were greater than the corresponding room temperature failure loads.

CONCLUSIONS

1. A7F maintains shear strength of 8.3 MPa (1200 psi) after exposure to environmental conditions.
2. A7F maintain flatwise tension strength above 11.0 MPa (1600 psi) at 561K (550°F).
3. CTE data for A7F adhesive shows a significant drop after aging.
4. Single-lap joints with preformed adherends showed a large increase in strength.
5. Adding a fabric interface between single-lap joint adherends, either S-glass/PI or Gr/PI, results in a significant increase in joint strength.
6. Scalloping the adherends of a single-lap joint does not significantly improve joint strength.
7. Graphite polyimide joints will carry loads of the magnitude expected for advanced aerospace vehicles at temperatures from 116K (-250°F) to 561K (550°F).
8. The weak link in joint strength was the low transverse tension strength of the composite.

REFERENCES

1. St. Clair, T. L.; and Progar, B. J.: LARC-13 Polyimide Adhesive Bonding. SAMPLE Series Volume 24—The Enigma of the Eighties: Environment, Economics, Energy. San Francisco. May 1979, pp. 1081-1092.
2. Sheppard, C. H.; Hoggatt, J. T.; and Symonds, W. A.: Quality Control Development for Graphite/PMR-14 Polyimide Composite Materials. NASA CR-159182, 1979.
3. Cushman, J. B.; and McCleskey, S. F.: Design Allowables Test Program, Celion 3000/PMR-15 and Celion 6000/PMR-15, Graphite/Polyimide Composites. NASA CR-165840, 1982.
4. Sawyer, James Wayne; and Cooper, Paul A.: Analysis and Test of Bonded Single Lap Joints with Preformed Adherends. AIAA/ASME/ASCE/AHS 21st Structures, Structural Dynamics and Materials Conference. May 1980, pp. 664-673.

ORIGINAL FILED
OF POOR QUALITY

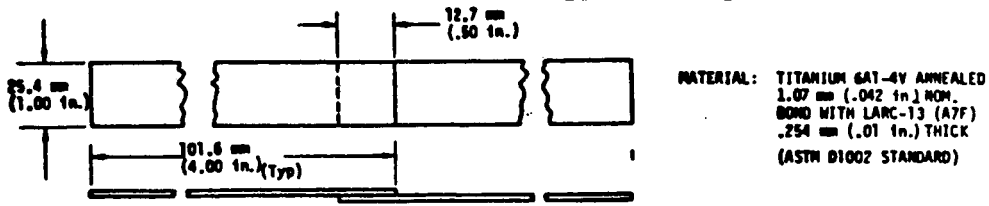


Figure 1: Titanium Single Lap Shear Specimen

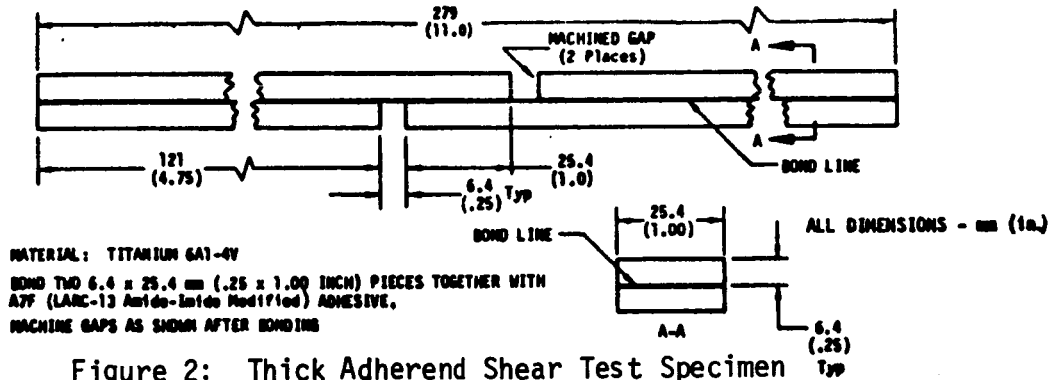


Figure 2: Thick Adherend Shear Test Specimen

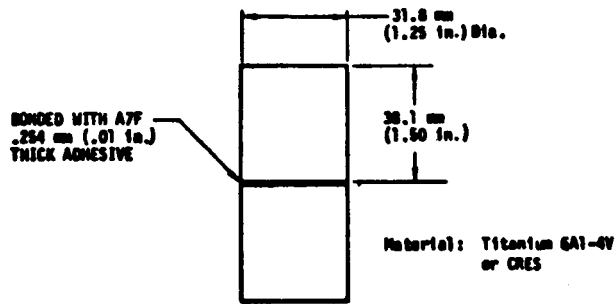


Figure 3: Flatwise Tension Adhesive Test Specimen

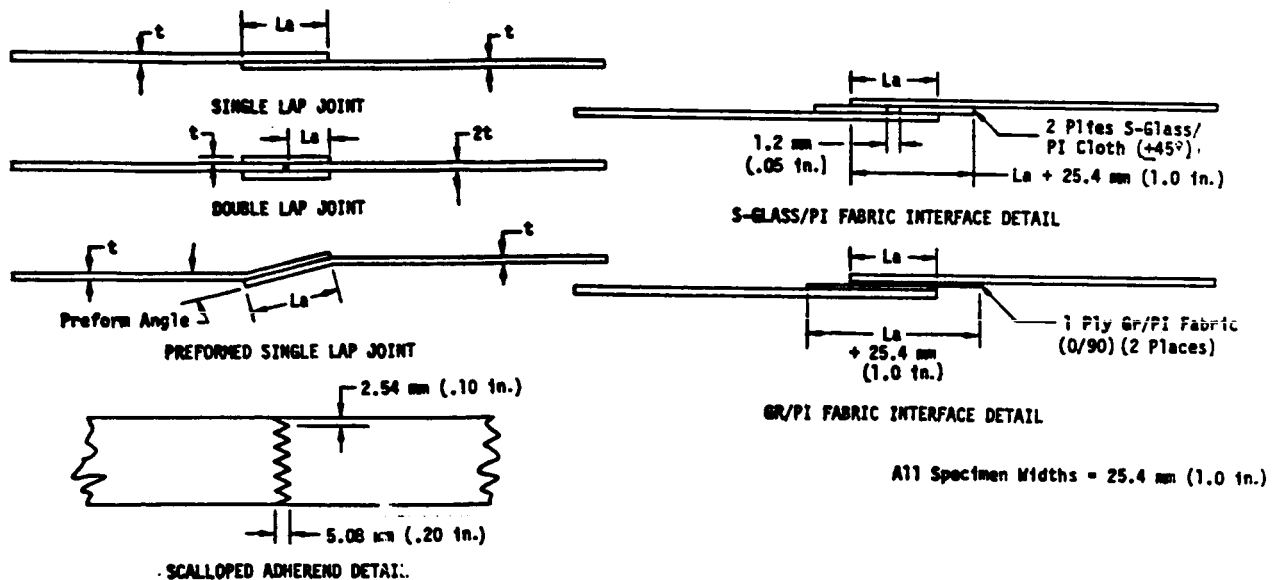
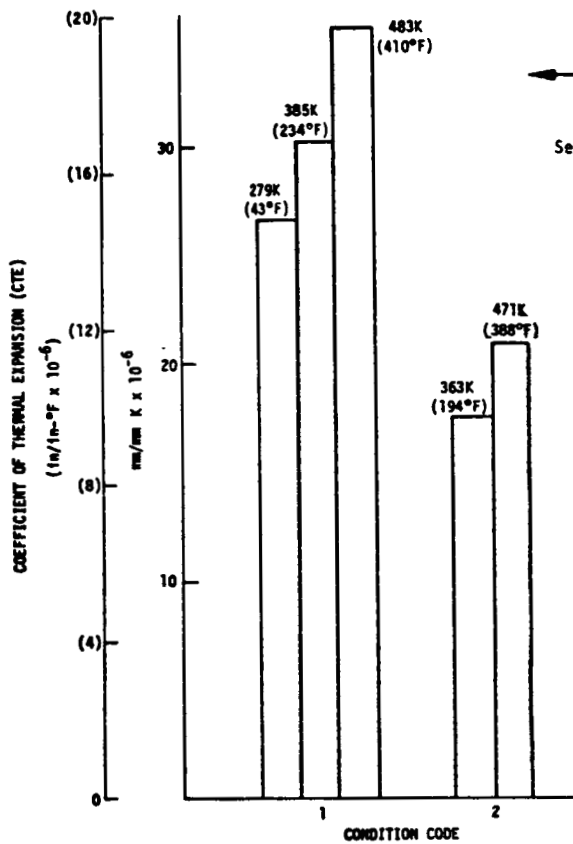


Figure 4: Advanced Joint Configurations



1. Cured/Post Cured
2. Aged 125 hrs. @ 589K (600)°F

Figure 5: Coefficient of Thermal Expansion--"A7F" Adhesive

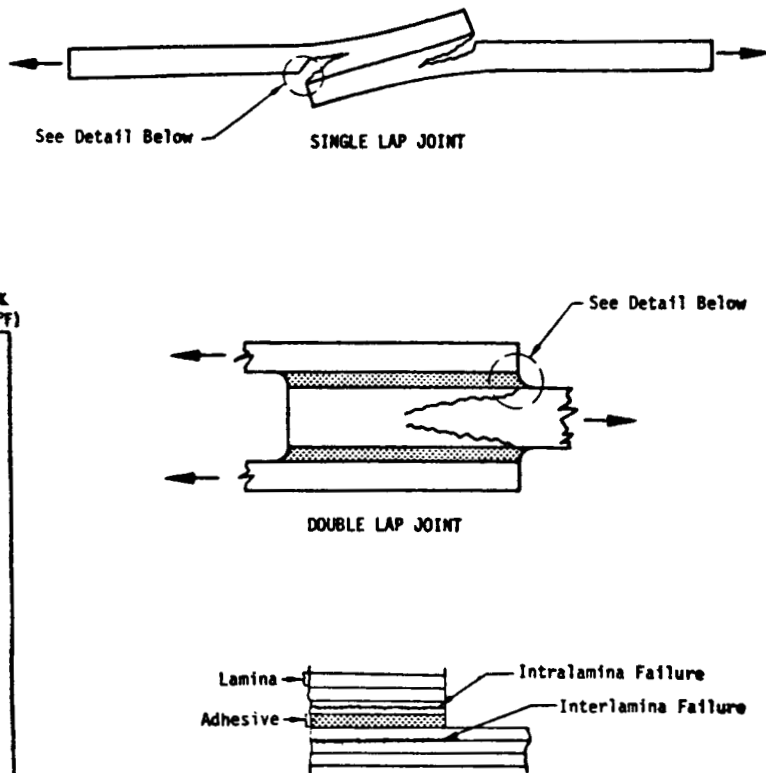


Figure 6: Peel Failures of Composite Bonded Joints

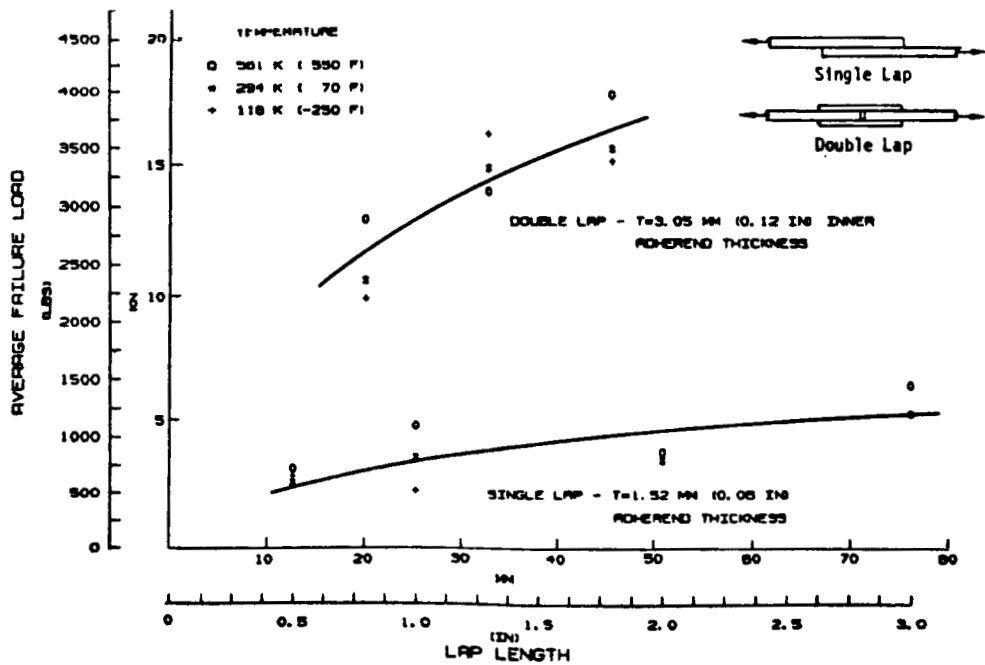


Figure 7: Comparison of Single- and Double-Lap Joints GR/PI to GR/PI Joints

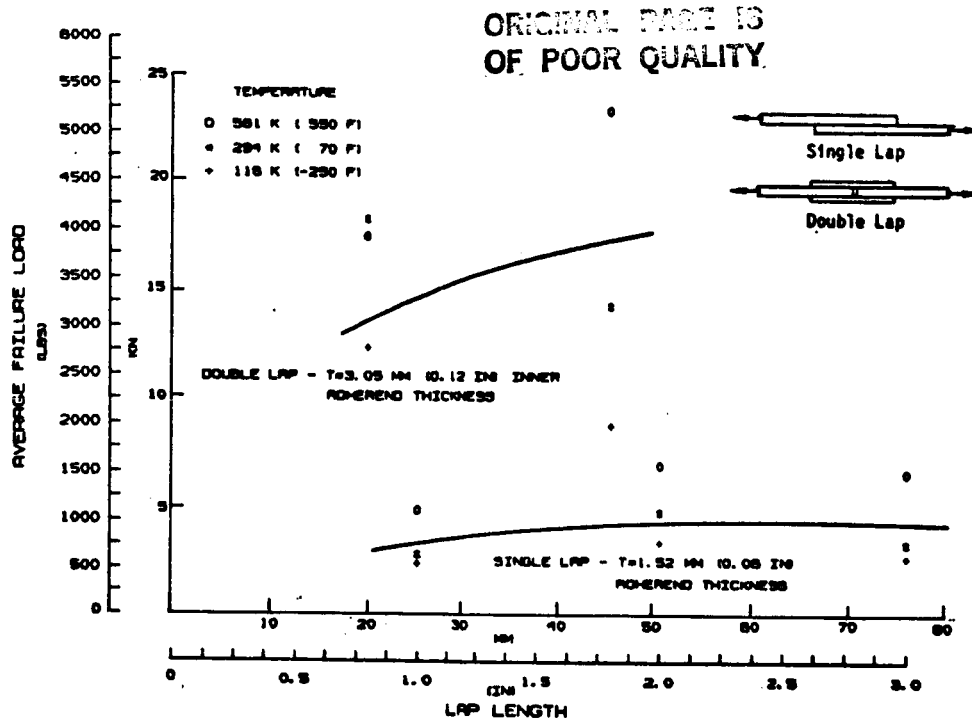


Figure 8: Comparison of Single- and Double-Lap Joints GR/PI to Titanium Joints

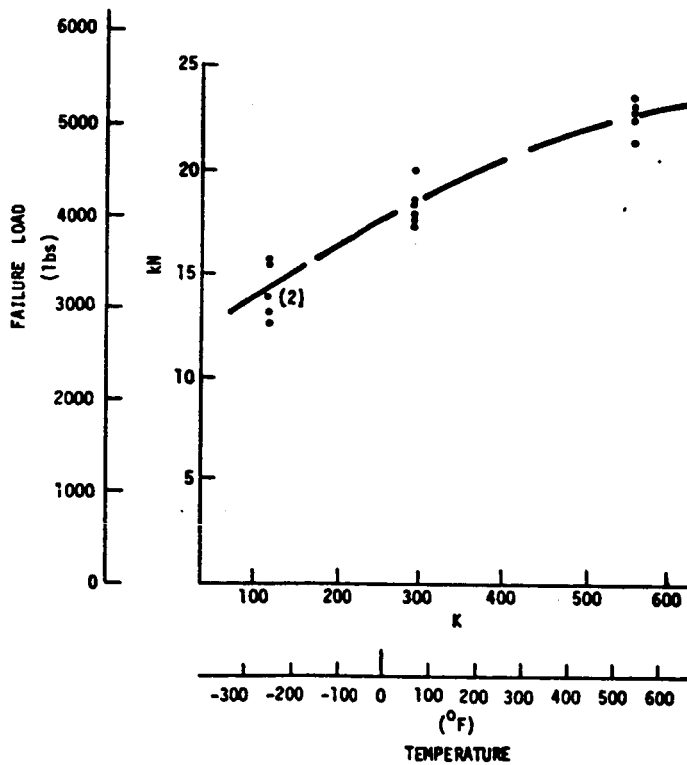


Figure 9: "3 Step" Symmetric Step-Lap Joint, GR/PI to Titanium

ORIGINAL PAGE IS
OF POOR QUALITY

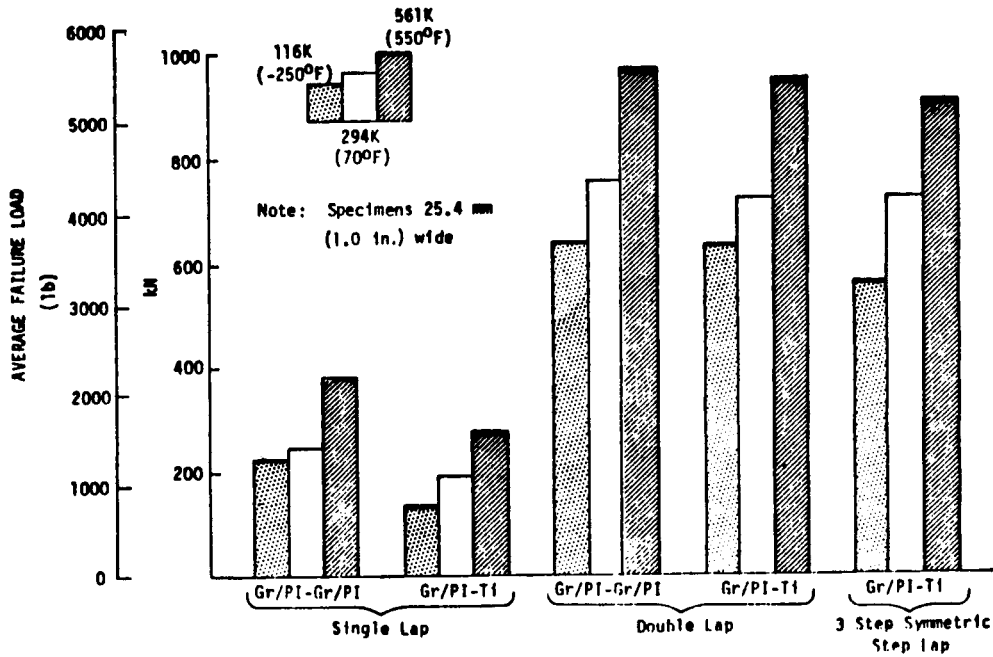


Figure 10: Maximum Joint Loads Achieved

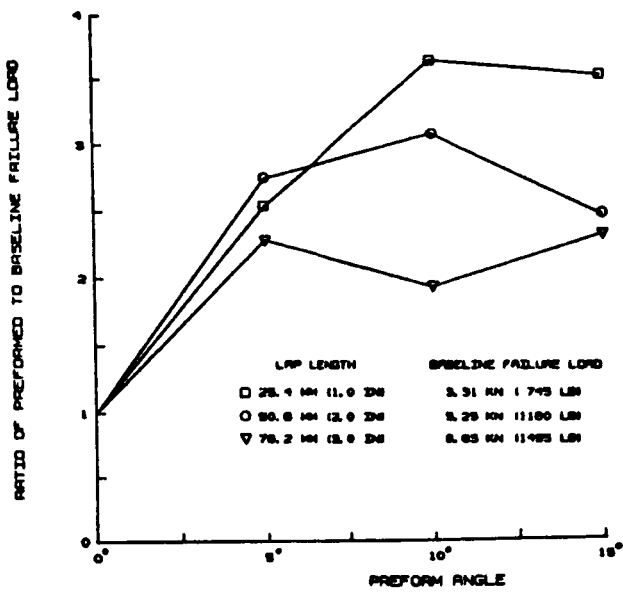


Figure 11: Effect of Preformed Adherends

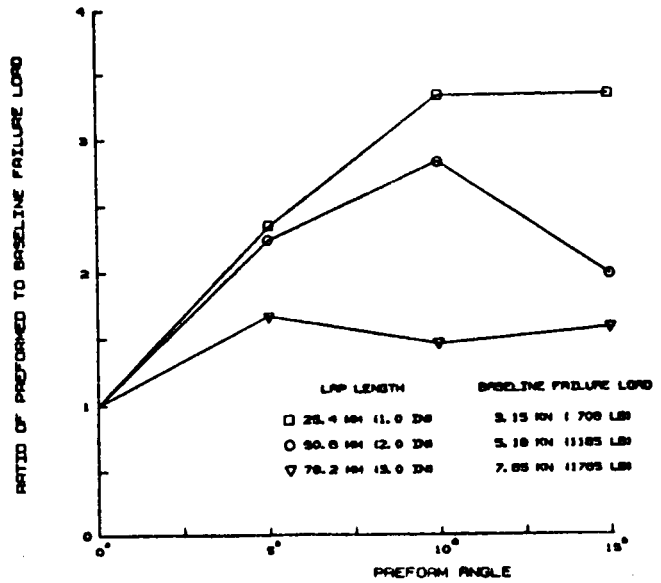


Figure 12: Effect of Preformed Adherends

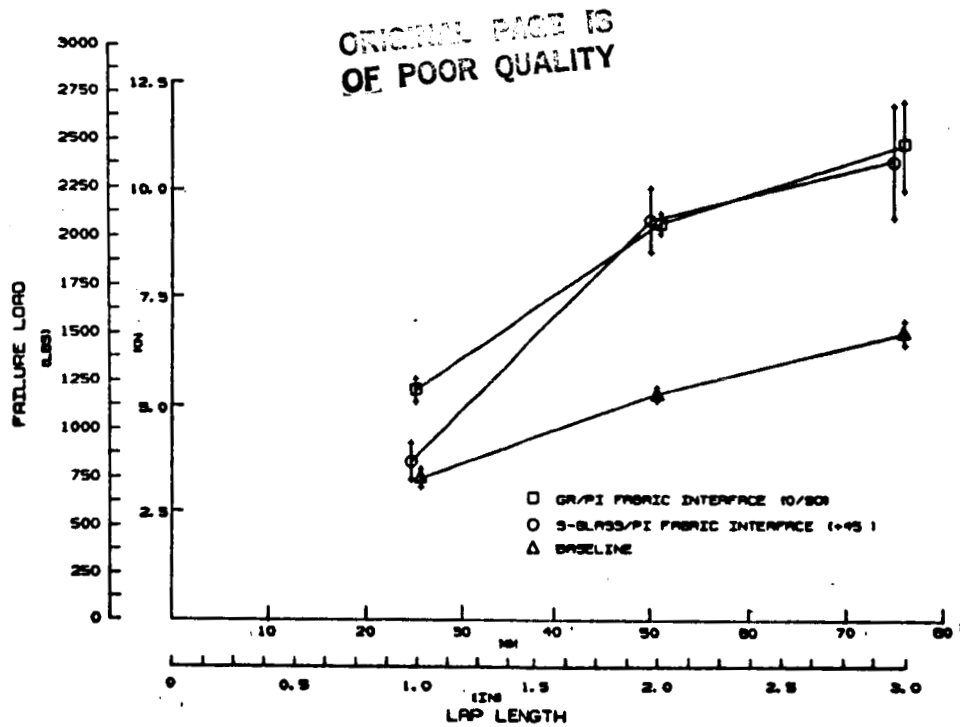


Figure 13: Effect of Fabric Interfaces - Single-Lap Joints

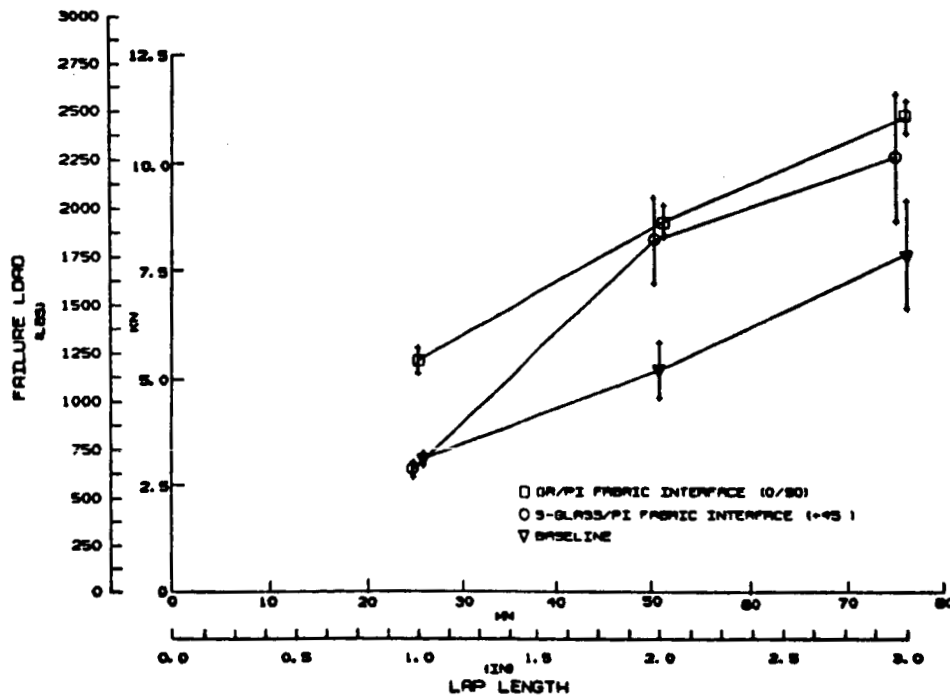


Figure 14: Effect of Fabric Interfaces - Single-Lap Joints

(a) SI Units

| CONDITIONING | TEMPERATURE K | LAP SHEAR ASTM D 1002 SHEAR STRENGTH MPa | "THICK ADHEREND" TESTS | | | FLATWISE TENSION STRENGTH MPa |
|----------------------------------------------------------|------------------|---------------------------------------------------|--------------------------|---------------------------|-----------------|----------------------------------------|
| | | | SHEAR STRENGTH MPa | SHEAR MODULUS MPa | SHEAR STRAIN | |
| Cured/ Post Cured | 116 | 20.7 | 22.57 | 61.83 | .7085 | 55.01 |
| | 294 | 19.67 | 16.72 | 70.37 | .4000 | 22.58 |
| | 561 | 13.53 | 8.79 | 45.82 | .4276 | 11.65 |
| Aged 125 hrs @ 589K (600°F) | 116 | 14.75 | 21.21 | 40.72 | .6305 | 45.15 |
| | 294 | 14.11 | 16.09 | 79.92 Intt. 53.53 Sec. | .5263 | 27.27 |
| | 561 | 14.34 | 13.33 | 52.70 | .4459 | 22.10 |
| Cycled 125 Times -116K (-250°F to 589K (600°F)) | 116 | 11.56 | — | — | — | — |
| | 294 | 12.18 | — | — | — | — |
| | 561 | 15.03 | — | — | — | — |

(b) US Customary Units

| CONDITIONING | TEMPERATURE F | LAP SHEAR ASTM D1002 SHEAR STRENGTH psi | "THICK ADHEREND" TESTS | | | FLATWISE TENSION STRENGTH psi |
|-----------------------------------------------------------|------------------|--------------------------------------------------|--------------------------|--------------------------|-----------------|----------------------------------------|
| | | | SHEAR STRENGTH psi | SHEAR MODULUS psi | SHEAR STRAIN | |
| Cured/ Post-Cured | -250 | 3003 | 3274 | 8968 | .7085 | 7978 |
| | 70 | 2853 | 2425 | 10206 | .4000 | 3275 |
| | 550 | 1963 | 1275 | 6645 | .4276 | 1690 |
| Aged 125 hrs @ 589K (600°F) | -250 | 2140 | 3076 | 5906 | .6305 | 6549 |
| | 70 | 2047 | 2333 | 11592 Intt. 7764 Sec. | .5263 | 3970 |
| | 550 | 2080 | 1933 | 7643 | .4459 | 3205 |
| Cycled 125 Times - 116K (-250°F) to 589K (600°F) | -250 | 1676 | — | — | — | — |
| | 70 | 1767 | — | — | — | — |
| | 550 | 2180 | — | — | — | — |

Table 1: Average Test Results For A7F Adhesive

| SPECIMEN CONFIGURATION | TEST NO. | LAP LENGTH mm (in.) | FAILURE MODE NUMBERS | | |
|---------------------------|-------------|---------------------------|----------------------|-------------|--------------|
| | | | 116K (-250°F) | 294K (70°F) | 561K (550°F) |
| 5° Preformed | 1a | 25.4 (1.0) | 1 | 1 | 1 |
| | 1b | 50.8 (2.0) | 1 | 1 | 1 |
| | 1c | 76.2 (3.0) | 2 | 1 | 1 |
| 10° Preformed | 2a | 25.4 (1.0) | 1 | 1 | 1 |
| | 2b | 50.8 (2.0) | 3 | 2 | 2 |
| | 2c | 76.2 (3.0) | 3 | 2, 3 | 3 |
| 15° Preformed | 3a | 25.4 (1.0) | 1, 2 | 1 | 1 |
| | 3b | 50.8 (2.0) | 3, 4 | 3 | 3 |
| | 3c | 76.2 (3.0) | 4 | 4 | 1, 4 |

Failure
Mode No.

Failure Mode

- Intralamina failure in adherend first ply + adherend-adhesive interface failure
- Interlamina failure in adherend + some tensile failures of individual plies
- Interlamina failure through adherend + tensile failures of individual plies
- Tensile failure of adherend at preformed bend

Table 2: Preformed Adherend Failure Modes